This article is part of the

Proceedings of the 16th Minisymposium Verfahrenstechnik and 7th Partikelforum (TU Wien, Sept. 21/22, 2020)

Title:
Development of an internally circulating fluidized bed for catalytic methanation of syngas

Corresponding author:
Alexander Bartik (TU Wien - ICEBE), alexander.bartik@tuwien.ac.at

Date of submission:
10.08.20

Date of revision:
19.09.20

Date of acceptance:
21.09.20

Chapter ID:
MoV2-(04)

Length:
9 pages

ISBN (full book):
978-3-903337-01-5

Development of an internally circulating fluidized bed for catalytic methanation of syngas

Alexander Bartik[1*], Josef Fuchs[1], Stefan Müller[1], Hermann Hofbauer[1]

[1] Institute of Chemical, Environmental and Bioscience Engineering, TU Wien, Austria
*Corresponding Author, alexander.bartik@tuwien.ac.at

Keywords: Internally circulating fluidized bed, Catalytic methanation, Reactor design, Fluid dynamics

Abstract

In this work, an internally circulating fluidized bed reactor was proposed and designed for the catalytic methanation of syngas from the 100 kW_{th} dual fluidized bed gasification reactor at TU Wien. Additionally, first fluid dynamic investigations were carried out in order to determine characteristic pressures and the gas slip in the internally circulating fluidized bed. The results from the design of the reactor showed that a volume contraction in the reactor between 30-50% and a heat generation between 0.16 to 0.25 kW per kW of exit gas need to be considered in the thermodynamic equilibrium for a low temperature methanation process at 300 °C and 1 bar_a. Further technical and economic considerations resulted in the design of a fluidized bed with an outer diameter of 164 mm, which corresponds to a maximum feed gas volume flow of 6 m^3_{stp}/h and a maximum chemical energy of 15 kW in the exit gas for the chosen catalyst properties. The fluid dynamic investigations with an inert bed material showed that there is a clear correlation between the pressure difference between the draft tube and the annular region and the fluidization ratio. Additionally, the gas slip was shown to increase with a higher fluidization ratio as well as higher absolute fluidization velocities. Furthermore, the gas slip from the annular region to the draft tube was shown to be by an order of magnitude higher than the gas slip from the draft tube to the annular region.

Introduction

The global energy system clearly shows a transition from solid energy carriers via liquids to gaseous energy carriers. This trend can be observed throughout historical data and is also predicted for centuries to come [1]. Besides the mere transition from solids to gases, there is also a transition from fossil fuels towards renewable energy resources taking place today. Synthetic natural gas (SNG) is one possible energy carrier which combines both trends and therefore shows a relevant potential for the implementation in future energy systems [2].

The Biomass-to-Gas (BtG) route is a viable concept for the production of valuable secondary energy carriers, like SNG, on a fossil-free basis. A possible process route within the BtG concepts is the dual fluidized bed (DFB) gasification and the consecutive upgrading to SNG. The upgrading steps consist of a gas cleaning section, the catalytic methanation process itself and the purification of the methane-rich gas (raw-SNG) in order to fulfill the feed-in requirements of the natural gas grid. Within this process chain, there are still some technical and economical challenges which must be addressed in order to make this process competitive [3]–[5]. Some recent investigations already focus on the implementation of the process chain in different industrial settings to extend the fields of application and improve the economic performance. In [6], for example, the process is utilized in an integrated hot metal production plant to replace the natural gas demand which is currently covered with fossil natural gas. Another study investigated the production of SNG from sewage sludge as feedstock. The results showed that the process can be economically competitive due to the negative purchase price of sewage sludge [7].

In this work, the focus lies on the design of the methanation reactor where the highly exothermic methanation reactions take place. The most important equations describing the ongoing processes are the CO-methanation reaction,

$$CO + 3H_2 \rightleftharpoons CH_4 + H_2O \qquad \Delta H_R^{300} = -216\,\frac{kJ}{mol} \quad (1)$$

the reverse water gas shift reaction, and

$$CO_2 + H_2 \rightleftharpoons CO + H_2O \qquad \Delta H_R^{300} = 39\,\frac{kJ}{mol} \quad (2)$$

the CO_2-methanation reaction, which is implicitly defined by the linear combination of Eq.(1) and (2) [8].

$$CO_2 + 4H_2 \rightleftharpoons CH_4 + 2H_2O \qquad \Delta H_R^{300} = -177\,\frac{kJ}{mol} \quad (3)$$

Besides these species, the product gas of the DFB gasifier also contains higher hydrocarbons like ethylene (C_2H_4). The hydrogenation of C_2H_4 to methane can be written as:

$$C_2H_4 + 2H_2 \rightarrow 2CH_4 \qquad \Delta H_R^{300} = -209\,\frac{kJ}{mol} \quad (4)$$

There are more reaction equations which can be considered in a methanation process, but are irrelevant for the purpose of this paper. A more detailed thermodynamic analysis for this process route can be found in [9].

Commercially, only adiabatic fixed bed reactors are available today. This type of reactor is chosen because of the low construction effort for a single reactor and the low mechanical stress on the catalyst. However, there are some major drawbacks as well. Because of the highly exothermic methanation reactions, a reactor cascade with intermediate gas cooling and most of the time also product gas recycle is necessary. This in term increases the complexity of the overall process setup. In addition, the risk for catalyst deactivation by carbon depositions and/or coke formation is high. For these reasons, alternative reactor concepts have been investigated. Cooled fixed bed reactors, fluidized bed reactors, three-phase reactors and structured reactors have been proposed for this purpose. This variety of reactor concepts also lead to a wide range of reaction conditions. 250 °C to 700 °C and 1 bar_a to 87 bar_a have been applied. Every reactor concept benefits from certain advantages but also shows disadvantages compared to adiabatic fixed beds. Fluidized bed reactors, for example, distinguish themselves by the improved heat and mass transfer. Therefore, nearly isothermal operation conditions and a high conversion close to the thermodynamic equilibrium even at lower temperatures are possible. Also, the risk for catalyst deactivation by coke formation is reduced and no separate water gas shift reactor prior to the methanation is necessary. All of the above points allow a shorter gas cleaning section

and reduce the number of required methanation reactors to a minimum. However, a drawback of the fluidized bed methanation reactor is the high mechanical stress on the catalyst. More information on the different reactor types can be found in [8], [10]–[12].

There are two large-scale projects for the conversion of woody biomass to SNG based on the DFB gasification technology. The GoBiGas project (Gothenburg, Sweden) produced 20 MW_{SNG} from the product gas of a DFB gasifier and utilized the commercially available TREMP process from Haldor Topsøe with 4 adiabatic methanation reactors with intermediate cooling and product gas recycling at a pressure of 16 bar_a. Together with the gas cleaning, the gas pretreatment and the gas upgrading, 16 main process steps are implemented in this plant. The second large-scale project was the 1 MW_{SNG} plant in Güssing, Austria. This plant utilized a single fluidized bed methanation reactor and 10 main process steps were necessary for the production of SNG from the product gas of the DFB gasifier. The operating conditions in the reactor were about 380 °C and 1 bar_a [8], [13].

Some investigations have already been performed on fluidized bed methanation in small lab-scale test rigs. These investigations mainly focus on the assessment of the catalyst performance in fluidized beds with only a few millimeters in diameter [14], [15]. Other investigations in somewhat larger bubbling fluidized bed reactors, with a diameter of about 50 mm, were conducted by the Paul Scherrer Institute (PSI). Extensive studies on kinetics, carbon depositions and mass transfer phenomena were carried out. All investigations utilized a bubbling fluidized bed but hardly any considerations to the reactor design are mentioned [16]–[18]. Other studies propose advanced two-stage methanation processes with a fluidized bed methanation reactor as the first stage and a fixed bed reactor as the second stage. However, these process setups were only theoretically proposed but have not been experimentally investigated so far [19], [20]. Neubert on the other hand already carried out experiments in a two-stage methanation process with intermediate water condensation including a structured reactor as the first stage and a fixed bed reactor as the second stage and reached to required gas quality for grid feed-in in Germany [21].

In this paper an internally circulating fluidized bed (ICFB) methanation reactor for improved heat and mass transfer is proposed and designed. Additionally, first results of fluid dynamic investigations of the ICFB are presented. The reactor concept is developed for the purpose of investigating the methanation process with bottled gases on the one hand and with 'live gas' from the 100 kW_{th} DFB gasifier at TU Wien on the other hand.

Concept and methodology

Design

ICFB's have been studied and applied to various processes in the past and today. Because of the possibility to split the reactor in different reaction zones, it is used in coal and biomass gasification processes, for example. The development of the DFB technology at TU Wien is also based on an ICFB and has been optimized over the last three decades [22], [23].

The ICFB reactor usually consists of one reactor with two separated fluidized beds and/or reaction zones, which are connected by the circulation of the solid material between the two zones. One possibility to separate the fluidized beds is by the insertion of a draft tube, which divides the reactor into an inner cylindrical fluidized bed and an outer annular fluidized bed. A schematic diagram of such an ICFB is shown in Fig. 1. By the independently controllable gas supply to each fluidized bed, it is possible to create a circulation between the two zones. For example, if there is a higher fluidization velocity inside the draft tube than in the annular region, the solids will rise in the draft tube and traverse downwards in the outer fluidized bed (green arrows in Fig. 1). ICFB's with draft tube mainly distinguish themselves by the fluid velocity in the draft tube. If the velocity is low, such that the particles are not carried out of the fluidized bed, the result are two interconnected bubbling fluidized beds and the solid circulation works on the principle of an airlift pump. If the fluid velocity in the draft tube is well above the point of entrainment (u_{se}, se=significant entrainment), the particles are carried out of the draft tube and flow back into the outer zone by the widening of the reactor above the draft tube. This type is called fast internally circulating fluidized bed (FICFB). Besides this definition, ICFB's can be distinguished by the type of the gas distributor or by the type of connection between the two reactor zones [24]–[27].

The proposed reactor concept is designed according to the following design parameters. The minimum fluidization velocity (u_{mf}) (Eq. 5) and u_{se} (Eq. 6) are calculated according to Grace [28] and Bi and Grace [29], respectively.

$$u_{mf} = \frac{\mu}{\rho_g \, d_{SV}} \left(\sqrt{27.2^2 + 0.0408 \, Ar} - 27.2 \right) \tag{5}$$

$$u_{se} = \frac{\mu}{\rho_g \, d_{SV}} \, 1.53 \, Ar^{0.5} \tag{6}$$

Where Ar is the Archimedes number.

$$Ar = \frac{d_{SV}^3 \, \rho_g \, (\rho_p - \rho_g) \, g}{\mu^2} \tag{7}$$

In order to calculate these parameters, gas properties like the dynamic viscosity μ and the density ρ_g must be known under the prevailing reaction conditions. For this reason, a model in the process simulation software IPSEpro was implemented. In this software, the property data for all required substances are implemented. These substances are H_2, CO, CO_2, CH_4, H_2O, N_2 and C_2H_4. Besides the property data of the gases, also the property data of the solid bed material must be defined. The defined bed material has a Sauter diameter of $d_{SV} = 165 \, \mu m$ and a particle density of $\rho_p = 2000 \, kg/m^3$. These values resemble the Ni/Al_2O_3-catalyst, which was synthesized especially for the utilization in a fluidized bed. Another useful definition for the characterization of the two fluidized beds is the superficial velocity in relationship to u_{mf}. This relationship can be defined for both the inner (u_d/u_{mf}, i.e. draft tube) and the outer (u_a/u_{mf}, i.e. annular region) fluidized bed. Division of these two values leads to the fluidization ratio,

$$fluidization\ ratio = \frac{u_d/u_{mf}}{u_a/u_{mf}} = \frac{u_d}{u_a} \tag{8}$$

which characterizes the circulation between the fluidized beds. Furthermore, the reaction conditions in the design case are set to 300 °C and 1 bar_a. The low temperature is possible because of the superiority of the fluidized bed in terms of heat management. It allows a high conversion and thus a methane-rich gas in a single reactor unit. Atmospheric pressure is chosen because the DFB gasification process works under ambient pressure and the energy, which is required for the pressurization of the feed gas, is omitted. Additionally, thermodynamic calculations reveal that there is only a mild influence of pressure on the gas composition

especially at low temperatures [9]. The temperature of the feed gas at the inlet to the reactor is set to 250 °C.

For the design of the fluidized bed, it is important to consider the chemical reactions taking place in the reactor. Not only the gas composition changes during the methanation process, but also the volume contracts (see Eq. 1,3 and 4). In the case of methanation it has been reported that the reaction kinetics are fast and the thermodynamic equilibrium can be approached within the first few millimeters of the reactor height [30]. Both statements justify the use of the exit gas composition/properties and volume flow in the thermodynamic equilibrium for the fluid dynamic calculations of the fluidized bed. Four typical feed gas compositions were used for the design of the reactor.

- a stoichiometric mixture of H_2 and CO_2 (H_2:CO_2 = 4:1).
- a stoichiometric mixture of H_2 and CO (H_2:CO = 3:1).
- a typical product gas composition from the DFB steam gasification with wood as fuel and olivine as bed material (typ. product gas) [23].
- a typical product gas composition from the sorption enhanced reforming process (SER) [31].

Fluid dynamic investigations

In order to characterize the fluid dynamic behavior of the ICFB cold flow experiments are carried out. The investigations focus on the determination of the pressure difference between the draft tube and the annular region of the ICFB as well as the gas slip between the two regions. As bed material quartz sand with similar properties as the catalyst is used. It characterizes as a Geldart group B material with a Sauter diameter of $d_{SV} = 143\,\mu m$ and a particle density of $\rho_p = 2600\ kg/m^3$. Fig. 1 shows the location of the pressure measurements. In order to obtain the pressure difference in the upper gap the pressure in the annular region (p_a) is subtracted from the pressure in the draft tube (p_d). This difference is an indication for the circulation of the bed material between the two regions as stated in [24]. The measurements are carried out with Kalinsky DS2 pressure transmitters. The gas slip on the other hand has an influence on the superficial velocity in the fluidized beds as well as on the gas compositions. The latter is important if two different feed gas streams are introduced to the two fluidized bed regions. This would be the case if, for example, an advanced two-stage methanation process in one reactor is investigated. In this case, the feed gas could be introduced to the draft tube and the exit gas of the draft tube then could be recycled to the annular region with a partial water condensation in between. The gas slip can be determined by introducing a tracer gas to one of the fluidized beds and measuring the concentration of the tracer gas after the draft tube (y_d), the annular region (y_a) and in the inlet stream (y_i). In our case, the tracer gas was CO_2 and its concentration was measured with an Emerson NGA 2000 gas analyzer module. A CO_2 mass balance then leads to Eq. 9 and Eq. 10 for the gas slip from the draft tube to the annular region (S_a) and vice versa (S_d).

$$S_d = \dot{Q}_d \frac{y_i - y_d}{y_d} \tag{9}$$

$$S_a = \dot{Q}_d y_a \frac{y_d - y_i}{y_d(y_d - y_a)} + \dot{Q}_a y_a \frac{1}{y_d - y_a} \tag{10}$$

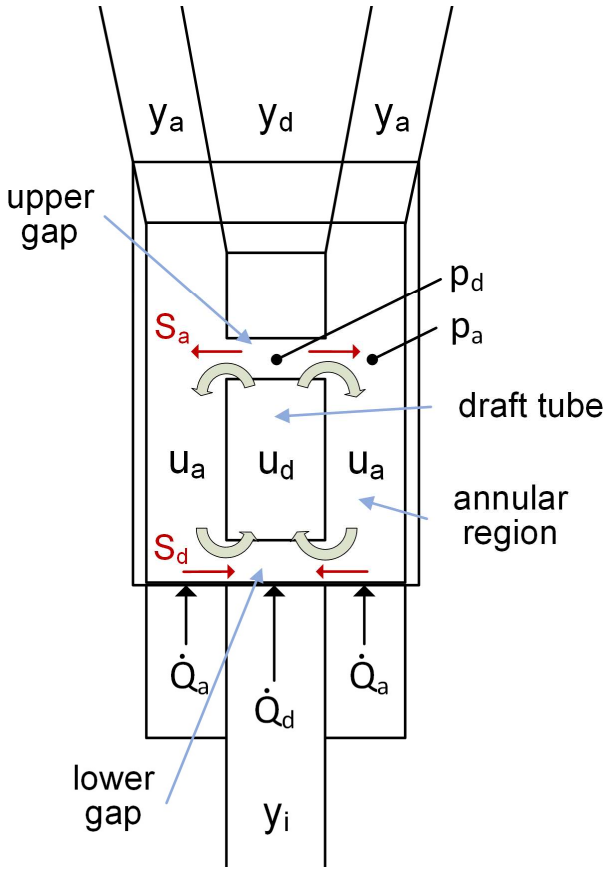

Figure 1: Schematic diagram of the ICFB reactor with bed material circulation (green arrows) and the direction of the gas slip (red arrows)

$\dot{Q}_d$ and $\dot{Q}_a$ denote the set volume flows to the draft tube and the annular region, respectively. All variables are also graphically represented in Fig. 1 and additionally also the direction of the gas slip is denoted with red arrows. The assumption that the gas slip to the draft tube (S_d) mainly takes place in the lower gap was experimentally confirmed in preliminary tests, while the assumption that the gas slip to the annular region (S_a) mainly takes place in the upper gap was shown to be a valid approximation in [24].

Results

Design

In Fig. 2a and Fig. 2b the feed gas composition and the equilibrium exit gas composition, respectively, are displayed for the four reference cases. The H_2:CO_2 feed gas mixture leads to an exit gas which consists mostly of CH_4 and H_2O. The latter can be easily condensed after the reactor but needs to be considered for the fluid dynamic design. The high water content can be explained by Eq. 3. It shows that two moles of H_2O are formed per mole of CO_2. The H_2:CO feed gas mixture shows a similar result, but with a higher CH_4 and a lower water content. For the typical product gas, the high CO_2 content is - besides CH_4 and H_2O - a relevant component for the fluid dynamic calculation. This is due to the understoichiometric hydrogen to carbon ratio of this feed gas. The SER product gas on the other hand produces an exit gas with a similar composition as the H_2:CO feed gas mixture. The CO in the feed gas is almost completely converted for all feed gases. In Fig. 2c the corresponding excess heat released by the exothermic reactions and the volume contraction for each feed gas mixture is depicted. The volume contraction is given in percent of the feed gas volume. The highest contraction takes place with the H_2:CO feed gas. The volume of the exit gas reduces to almost 50%

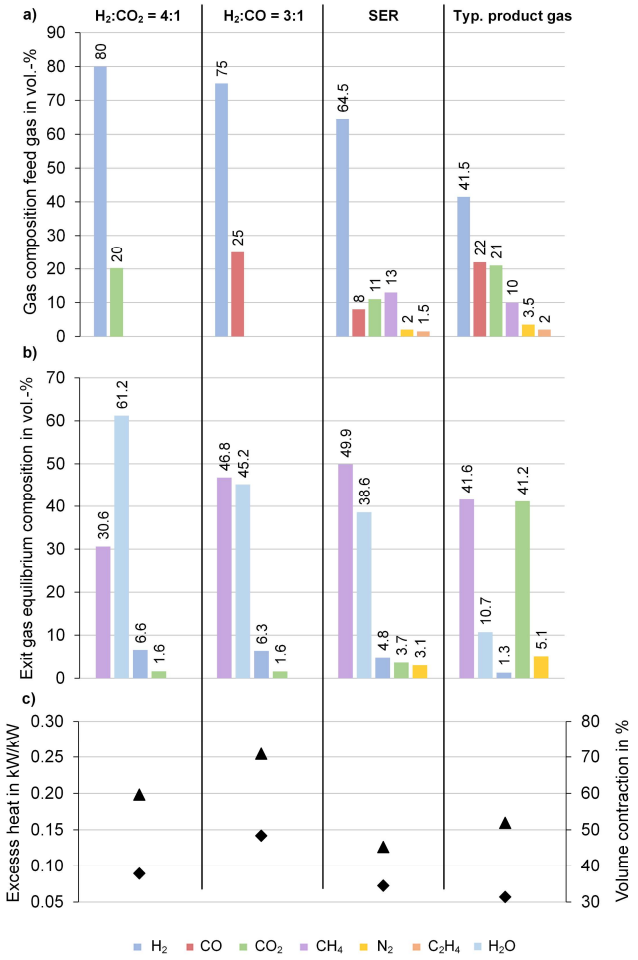

Figure 2: Gas compositions used for the design of the fluidized bed reactor: a) feed gas composition, b) exit gas composition according to the thermodynamic equlibrium at 300 °C and 1 bar_a, c) heat dissipation and volume contraction during the conversion of the feed gas to the exit gas

of the volume of the feed gas. The excess heat on the left axis indicates how much heat is released by the exothermic reactions and therefore needs to be removed by the reactor cooling to ensure an isothermal operation. It is given in kW per kW of chemical energy of the exit gas. The H_2:CO mixture leads to the highest amount of produced heat with about 0.25 kW/kW.

With this knowledge, it is possible to calculate the fluid dynamic parameters and in further consequence determine the plant size and the plant design. The calculation is done by varying the size parameters of the fluidized beds and checking the required volume flows and the fluidization ratio. Based on this iteration a decision for a plant size is made. Consequently, the results for these size parameters are shown. The diameter of the inner fluidized bed is 80 mm and the diameter of the annular fluidized bed is 164 mm. The decision for this size is based on the following limitations: i) the amount of gas in the feed must be covered by gas cylinders and is therefore limited because of economic considerations, ii) the excessive heat must be manageable in the reactor, iii) the amount of product gas from the 100 kW_{th} pilot plant must be sufficient (typically 20-30 Nm^3/h on a dry basis), iv) the size of the fluidized beds should not be below a certain scale limit in order to have a representative size for further upscaling considerations. Table 1 shows the results of this calculation. u_{mf} and u_{se} as

Table 1: U_{mf} and U_{se} as well as calculation results for the four investigated feed gas compositions and three different fluidization ratios

Parameter	Unit	Gas compositions			
		H_2:CO_2 = 4:1	H_2:CO = 3:1	SER	Typ. prod. gas
U_{mf}	cm/s	2.0	2.03	1.98	1.68
U_{se}	cm/s	464	468	454	358
$\boldsymbol{U_d/U_a = 5/2}$					
Volume flow feed	Nm^3/h	2.76	3.36	2.59	2.08
Excess heat	kW	1.1	2.14	1.1	0.96
Chem. Energy exit gas	kW	5.54	8.41	8.64	6.02
$\boldsymbol{U_d/U_a = 10/3}$					
Volume flow feed	Nm^3/h	4.82	**5.88**	4.53	3.66
Excess heat	kW	1.92	**3.74**	1.91	1.68
Chem. Energy exit gas	kW	9.68	14.7	**15.1**	10.53
$\boldsymbol{U_d = U_{se}, U_a = 0}$					
Volume flow feed	Nm^3/h	63.6	77.1	59.1	44.3
Excess heat	kW	25.35	49	25	20.3
Chem. Energy exit gas	kW	127.8	193	197	127.4

well as the chosen fluidization ratios, the required volume flows of the feed gas, the excess heat, which is produced by the exothermic reactions, and the chemical energy of the exit gas (i.e. the raw-SNG) are listed for the four previously defined feed gas compositions. The fluidization ratio of 5/2 represents the standard design case and the fluidization ratio of 10/3 the maximum design case. The resulting maximum values are displayed in bold numbers. The maximum volume flow of 5.88 Nm^3/h of feed gas for the

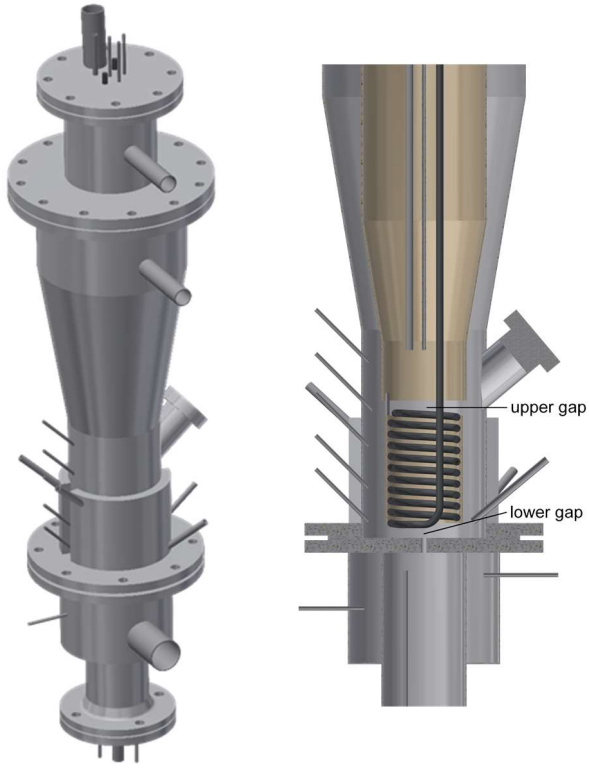

Figure 3: 3D-CAD drawing of the ICFB reactor: isometric view of the whole reactor (left), sectional view of the lower reactor part (right)

H_2:CO mixture can be covered from gas cylinders. This list also shows that the reactor cooling must dissipate a maximum of 3.74 kW. In the last section of the table, values

for the design of a FICFB are given. In this case, the velocity in the draft tube is equal to u_{se}. The resulting volume flows and the excess heat are by an order of magnitude higher than in the previous cases. This volume flow can neither be covered by gas cylinders nor by the DFB pilot plant. Vice versa, if the volume flows are reduced to a manageable level, the reactor diameter is considered too small for a representative operation. Therefore, the design and construction of a FICFB is not expedient in this case.

Based on these calculations a 3D-CAD drawing of the ICFB reactor is created. The left picture in Fig. 3 shows the complete reactor from the outside. The lowest part of the drawing shows the two windboxes, which allow an individual gas flow to the two fluidized beds. The flange above the windbox incorporates the gas distributor, which is in this case made of 22 pneumatic silencers. This flange connects to the actual reactor zone where the reaction takes place. Above the reaction zone are two conical freeboards – one for the annular fluidized bed and one for the draft tube. The gas streams then leave the reactor by two separate pipes.

In the right part of Fig. 3, a section view of the lower reactor part is shown. The bed material is fluidized and the reaction takes place in the depicted area above the gas distributor. In order to manage the heat released by the exothermic reactions, the draft tube is cooled by an air perfused coil. Below and above the draft tube the gap for the bed material circulation can be seen (upper gap and lower gap). A cooling jacket on the outside of the reactor additionally cools the annular part of the ICFB with air. The air crisscrosses several times in the cooling jacket before it is exhausted. The exiting raw-SNG can be separately withdrawn from the reactor through the inner pipe and the outer conical annular region.

Subsequently a P&I diagram of the whole process setup is drafted based on the results from the calculations and the 3D-CAD drawing (Fig. 4). All temperature, pressure, gas volume flow and gas measurement points are displayed in the flowchart. The plant is equipped with a maximum of 10 pressure and 29 temperature measurement points. Also, 5 gas measurement points for the measurement of the gas

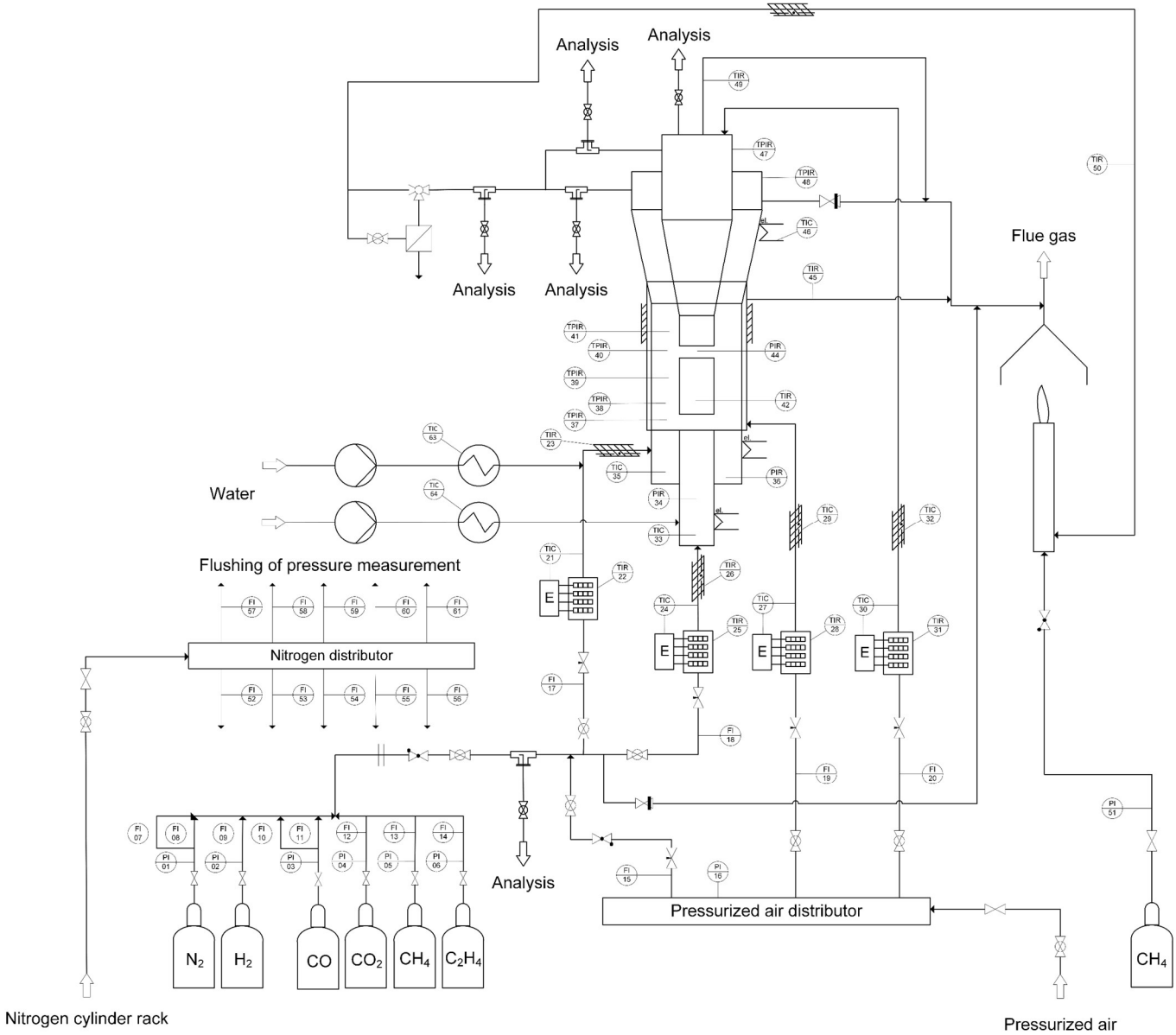

Figure 4: P&I flowchart of the process setup

The various small pipes coming off of the reactor are used for the installation of temperature sensors as well as connection points for pressure or gas measurements.

composition with online measuring devices are included (denoted by 'Analysis' in the flowchart). All pressure measurement points are flushed with a small amount of nitrogen to protect the pressure transmitters and to clear the pipes from reacting gases and bed material. In the bottom left corner of the flowchart, the gas cylinders are depicted. The volume flows of the single gas components are controlled by variable area flow meters (also called rotameters) with an integrated needle valve. The mixed gas is then split up into two streams in order to supply the gas flow to the draft tube and the annular fluidized bed. Again, rotameters are used to set the split ratio between the two regions. The composition of the mixed feed gas can be verified at the point marked with 'Analysis'. Afterwards the feed gas streams are preheated to 250 °C (design case) by electrical heating cartridges. Additionally, heating tapes are used to equalize the heat losses in the pipes from the heating cartridges to the reactor. In the reactor itself, temperature, pressure and gas measurement points are installed over the height of the annular fluidized bed in order to obtain axial profiles. In the draft tube the measurement is carried out by vertically moveable pipes which also yield axial profiles. At the two exits of the reactor, the composition of the two gas streams from the draft tube and the annular zone can be measured separately. These two gas streams are then mixed and the gas composition can be measured again. Afterwards, the gas flows through a filter stuffed with glass wool. The plant parts after the reactor are also equipped with heating tapes in order to prevent water condensation. A bypass allows changing the filter material during operation, if any problems should arise. The exit gas is then directed to a natural gas operated torch where the raw-SNG is burnt. Eventually, the flue gases are ventilated through a chimney. At the bottom center of the flowchart the pressurized air supply for the reactor cooling is depicted. Again, rotameters with a needle valve control the volume flow of the cooling air. For the plant start-up phase, the air can be preheated the same way the feed gas is preheated. The cooling air leaving the reactor is also ventilated through the chimney. In order to enable the water-gas shift reaction, water vapor can be dosed individually to the two fluidized beds. Additionally, the installation of two safety valves ensure a safe operation of the plant.

The shown configuration in Fig. 4 is designed and constructed for the operation with gas cylinders and 'live-gas' from the DFB pilot plant at TU Wien. The latter case is not shown in the flowchart. Regarding the construction of the plant, there is, however, no change necessary. The flowchart also shows that the separate exit gases from the draft tube and the annular zone are merged together after the reactor. This can be easily adapted for the investigation of a two-stage methanation process. The exit gas from the annular zone can be recirculated to the draft tube by the installation of a recirculation pipe as well as a blower. Additionally, a partial water condensation in the recirculation pathway can be installed. Both measures possibly allow an enhanced conversion of the feed gas to methane.

In Fig. 5, a picture of the bench-scale ICFB methanation setup at TU Wien is shown. The picture shows the plant without insulation and without heating tapes. On the right, the connection points to the gas cylinders and the pressurized air are located. Here, also the rotameters for the feed gas splitting and the cooling air are shown. On the left middle the actual ICFB reactor is placed. The exhaust gas pathway follows to the left of the reactor. The pressure transmitters and the electrical installations are located on the back of the plant in the control cabinet. Each of the 4 heating cartridges has an installed electrical power of 1.2 kW. Together with the heating tapes and the water evaporators, the plant has a maximum installed electrical power of about 11.5 kW.

Figure 5: Picture of the bench-scale methanation setup at TU Wien

Fluid dynamic investigations

In Fig. 6 the pressure difference in the upper gap between the draft tube and the annular region is shown over the fluidization ratio u_d/u_a. In the P&I flowchart, the corresponding pressure measurement points are PIR44 and PIR40. The graph shows that the pressure difference increases with an increasing fluidization ratio. With a high accuracy, this relationship is shown to be of a quadratic nature and can be seen as an indication for the bed material circulation rate. Additionally, also the absolute fluidization velocities influence the pressure difference. I.e. a higher u_a and therefore also a higher u_d lead to a higher pressure difference at a constant fluidization ratio. These results are in accordance with [24], who also found that the pressure difference gives an indication for the bed material circulation rate.

Fig. 7 shows the gas slip from the draft tube to the annular region (S_a) in Nm^3/h over the fluidization ratio u_d/u_a for different fluidization velocities (u_a=1.5-3.9u_{mf}) and two different sand filling levels. In Fig. 7a, the sand completely

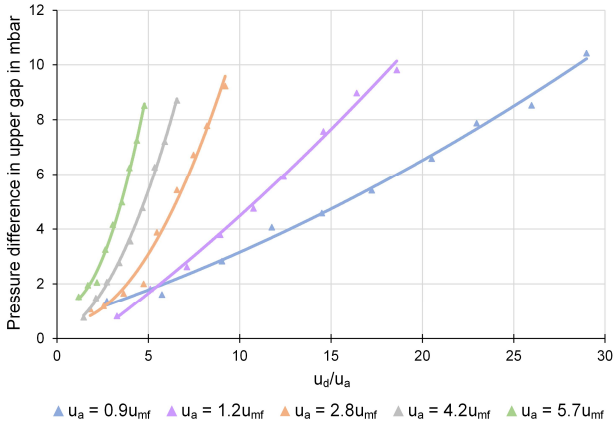

Figure 6: Pressure difference in the upper gap over the fluidization ratio

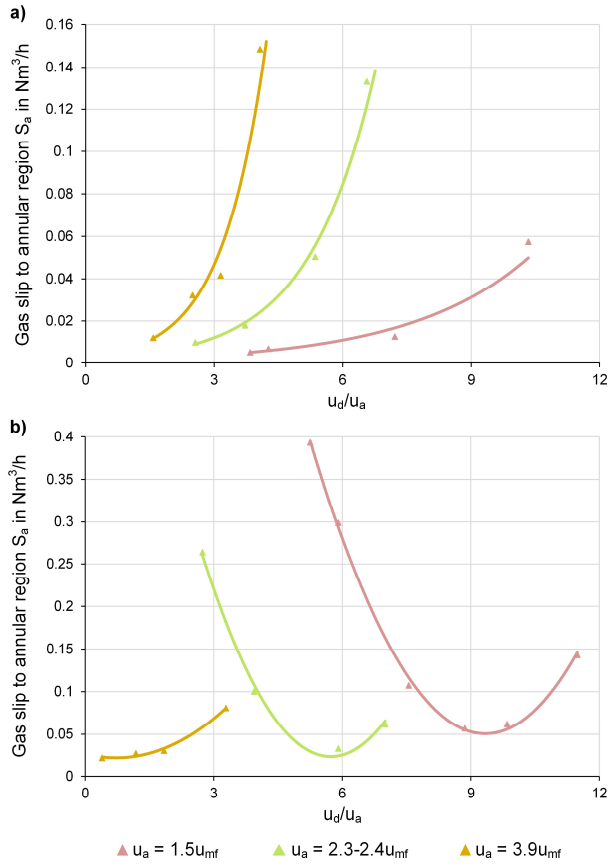

Figure 7: Gas slip to the annular region (S_a) over the fluidization ratio for different u_a: a) sand covers the upper gap completely, b) sand covers the upper gap only partially

covers the upper gap even when the reactor is not fluidized, while in Fig. 7b the upper gap is not completely covered with sand as long as the reactor is not fluidized.

The results for the fully covered gap in Fig. 7a show a steep incline of the gas slip with a rising u_d/u_a. The rising gas slip is in accordance with the increasing pressure difference in the upper gap (cf. Fig. 6). This increased pressure leads to a higher bed material circulation rate and simultaneously also pushes the gas from the draft tube to the annular region. Besides the influence of the fluidization ratio, also the absolute fluidization velocities determine the gas slip to a large extent. Like the pressure difference, higher fluidization velocities lead to a higher gas slip. Between $5*10^{-3}$ and 0.15 Nm^3/h, which is equal to a relative gas slip between 0.4 to 5 % of $\dot{Q}_a$, slip to the annular region. In Fig. 7b on the contrary, the only partially covered upper gap leads to a much higher gas slip compared to the fully covered gap, because the gas is able to flow from the draft tube to the annular region without resistance from the bed material. With an increasing fluidization ratio (for $u_a=1.5u_{mf}$ and $u_a=2.4u_{mf}$), the gas slip decreases because the bed material expands further and therefore also the gap closes gradually. At a certain fluidization ratio, the gap is fully closed and the gas slip increases again with higher fluidization ratios. If the absolute fluidization velocities are high enough in order to cover the gap even at low fluidization ratios (e.g. $u_a=3.9u_{mf}$), the course of the curve is similar to the curves in Fig. 7a.

The gas slip from the annular region to the draft tube S_d does not show such a clear correlation with the fluidization ratio as S_a. Nevertheless, it could be shown that S_d ranges between 0.1 and 0.76 Nm^3/h, which is equal to a relative gas slip between 4 to 43% of $\dot{Q}_a$. Hence, S_d is almost an order of magnitude higher than S_a and thus has a significant impact on the fluidization velocity and the gas composition in the draft tube. These results are again in accordance with Hofbauer [24] who also found that S_d is much higher than S_a.

Conclusion and Outlook

In this work, an ICFB has been proposed and designed for the optimized catalytic methanation of syngas from the DFB gasification process. Additionally, first results from fluid dynamic investigations in the ICFB have been presented. The application of a fluidized bed shows advantages in terms of heat management, conversion efficiencies and the prevention of catalyst fouling by coke depositions. Additionally, the whole process setup of the BtG process route is simplified. This work has shown, that the design of an ICFB for catalytic methanation requires careful thermodynamic modelling (Fig. 1). Besides the different gas compositions and properties, also the volume contraction of the gas during methanation must be considered. Additionally, the heat evolution by the exothermic reactions must be modelled in order to design a suitable cooling system to ensure an isothermal operation of the fluidized bed. The consideration of different operating conditions has been used to determine the plant size and point out the limits of a technical and economical operation (Table 1). These considerations have resulted in a novel reactor design for the production of maximum 15 kW of raw-SNG from about 6 Nm^3/h of syngas. Additionally, fluid dynamic investigations have shown that the pressure difference in the upper gap between the draft tube and the annular region is proportionate to the fluidization ratio and most likely also to the bed material circulation rate. The determination of the gas slip between the two fluidized beds has also shown a clear correlation with the fluidization ratio. A completely covered upper gap has been shown to be essential for a minimal gas slip. Simultaneously, the gas slip from the annular region to the draft tube has been found to be by an order of magnitude higher than the gas slip from the draft tube to the annular region. Further investigations concerning the fluid dynamics should focus on the determination of the gas slip from the annular region to the draft tube and on the quantification of the bed material circulation rate. With respect to the actual methanation, the designed ICFB reactor will be used to investigate the methanation reactions with syngas from gas cylinders. Additionally, the plant will be integrated into the whole BtG process chain, where it is connected to the 100 kW_{th} DFB pilot plant and a gas cleaning section in order to demonstrate 'live-gas' methanation.

Acronyms

BtG	biomass-to-gas
CAD	computer aided design
DFB	dual fluidized bed
FICFB	fast internally circulating fluidized bed
ICFB	internally circulating fluidized bed
SER	sorption enhanced reforming
SNG	synthetic natural gas

Symbols

Ar	Archimedes number
d_{SV}	Sauter diameter in μm

u_a	superficial velocity in the annular fluidized bed in cm/s
u_d	superficial velocity in the draft tube in cm/s
u_{mf}	minimum fluidization velocity in cm/s
u_{se}	velocity where significant entrainment occurs (= fast fluidized bed) in cm/s
μ	dynamic viscosity in Pas
ρ_g	density of the gas in kg/m^3
ρ_p	particle density in kg/m^3
S_a	gas slip from the draft tube to the annular region in Nm^3/h
S_d	Gas slip from the annular region to the draft tube in Nm^3/h
$\dot{Q}_a$	volume flow to annular region in Nm^3/h
$\dot{Q}_d$	volume flow to annular region in Nm^3/h
y_a	volume fraction of CO_2 above the annular fluidized bed
y_d	volume fraction of CO_2 above the draft tube
y_i	volume fraction of CO_2 in the feed gas

Acknowledgement

This work is part of the research project ReGas4Industry (871732) and receives financial support from the research program "Energieforschung" funded by the Austrian Climate and Energy Fund.

References

[1] S. Dunn, "Hydrogen futures: Toward a sustainable energy system," Int. J. Hydrogen Energy, vol. 27, no. 3, pp. 235–264, 2002.
[2] European Commission, "Directive (EU) 2018/2001 of the European Parliament and of the Council of 11 December 2018 on the promotion of the use of energy from renewable sources," Off. J. Eur. Union, vol. L 328/82, no. December, p. 128, 2018.
[3] D. Hornbachner, G. Hutter, and D. Moor, "Biogas-Netzeinspeisung - Rechtliche, wirtschaftliche und technische Voraussetzungen in Österreich," 2005.
[4] A. Larsson, I. Gunnarsson, and F. Tengberg, "The GoBiGas Project - Demonstration of the Production of Biomethane from Biomass via Gasification", Technical Report, 2018.
[5] J. Karstensson, A. Eliasson, and A. Kronander, "Feasibility study for gasification of biomass for synthetic natural gas (SNG) production," 2015. doi: 10.13140/RG.2.1.4321.6245
[6] S. Müller, L. Theiss, B. Fleiß, M. Hammerschmid, J. Fuchs, S. Penthor, D.C. Rosenfeld, M. Lehner and H. Hofbauer, "Dual Fluidized Bed Based Technologies for Carbon Dioxide Reduction – Example Hot Metal Production", accepted for publication in Biomass Conv. Bioref., 2020
[7] M. Veress, A. Bartik, F. Benedikt, M. Hammerschmid, J. Fuchs, S. Müller and H. Hofbauer, "Development and techno.economic evaluation of an optimized concept for industrial bio-SNG production from sewage sludge", Proceedings of the 28th European Biomass Conference, 2020
[8] T. J. Schildhauer and S. M. A. Biollaz, Synthetic Natural Gas from Coal, Dry Biomass, and Power-to-Gas Applications. Hoboken: John Wiley & Sons, 2016.
[9] A. Bartik, F. Benedikt, A. Lunzer, C. Walcher, S. Müller, and H. Hofbauer, "Thermodynamic Investigation of SNG Production Based on Dual Fluidized Bed Gasification of Biogenic Residues", Biomass Conv. Bioref., 2020. doi: 10.1007/s13399-020-00910-y
[10] J. Kopyscinski, T. J. Schildhauer, and S. M. A. Biollaz, "Production of synthetic natural gas (SNG) from coal and dry biomass - A technology review from 1950 to 2009," Fuel, vol. 89, no. 8, pp. 1763–1783, 2010. doi: 10.1016/j.fuel.2010.01.027
[11] T. J. Schildhauer and S. M. A. Biollaz, "Reactors for catalytic methanation in the conversion of biomass to synthetic natural gas (SNG)," Chimia, vol. 69, no. 10, pp. 603–607, 2015. doi: 10.2533/chimia.2015.603
[12] S. Rönsch et al., "Review on methanation – From fundamentals to current projects," Fuel, vol. 166, pp. 276–296, 2016. doi: 10.1016/j.fuel.2015.10.111
[13] B. Rehling, "Development of the 1MW Bio-SNG plant , evaluation on technological and economical aspects and upscaling considerations," Dissertation, 2012.
[14] J. Li et al., "Enhanced fluidized bed methanation over a Ni/Al2O3 catalyst for production of synthetic natural gas," Chem. Eng. J., vol. 219, pp. 183–189, 2013. doi: 10.1016/j.cej.2013.01.005
[15] B. Liu and S. Ji, "Comparative study of fluidized-bed and fixed-bed reactor for syngas methanation over Ni-W/TiO2-SiO2 catalyst," J. Energy Chem., vol. 22, no. 5, pp. 740–746, 2013. doi: 10.1016/S2095-4956(13)60098-4
[16] J. Kopyscinski, T. J. Schildhauer, and S. M. A. Biollaz, "Fluidized-bed methanation: Interaction between kinetics and mass transfer," Ind. Eng. Chem. Res., vol. 50, no. 5, pp. 2781–2790, 2011. doi: 10.1021/ie100629k
[17] M. C. Seemann, T. J. Schildhauer, S. M. A. Biollaz, S. Stucki, and A. Wokaun, "The regenerative effect of catalyst fluidization under methanation conditions," Appl. Catal. A Gen., vol. 313, no. 1–2, pp. 14–21, 2006. doi: 10.1016/j.apcata.2006.06.048
[18] M. C. Seemann, T. J. Schildhauer, and S. M. A. Biollaz, "Erratum: Fluidized bed methanation of wood-derived producer gas for the production of synthetic natural gas", Ind. Eng. Chem. Res., vol. 49, no. 15, p. 7034-7038, 2010. doi: 10.1021/ie100510m
[19] J. Liu, D. Cui, C. Yao, J. Yu, F. Su, and G. Xu, "Syngas methanation in fluidized bed for an advanced two-stage process of SNG production," Fuel Process. Technol., vol. 141, pp. 130–137, 2016. doi: 10.1016/j.fuproc.2015.03.016
[20] J. Witte, J. Settino, S. M. A. Biollaz, and T. J. Schildhauer, "Direct catalytic methanation of biogas – Part I: New insights into biomethane production using rate-based modelling and detailed process analysis," Energy Convers. Manag., vol. 171, no. December 2017, pp. 750–768, 2018. doi: 10.1016/j.enconman.2018.05.056
[21] M. Neubert, "Catalytic methanation for small- and mid-scale SNG production," Friedrich-Alexander Universität Erlangen-Nürnberg, Dissertation, 2019.
[22] H. Hofbauer, "Energy from Biomass via Gasification in Güssing," in Biomass Power for the World: Transformations to Effective Use, W. van Swaaij, S. Kersten, and W. Palz, Eds. Pan Stanford, 2015.
[23] J. C. Schmid, F. Benedikt, J. Fuchs, A. M. Mauerhofer, S. Müller, and H. Hofbauer, "Syngas for biorefineries from thermochemical gasification of lignocellulosic fuels and residues - 5 years' experience with an advanced dual fluidized bed gasifier design," Biomass Conv. Bioref., 2019. doi: 10.1007/s13399-019-00486-2

[24] H. Hofbauer, “Experimentelle Untersuchungen an einer zirkulierenden Wirbelschicht mit Zentralrohr,” TU Wien, Dissertation, 1982.
[25] B. J. Milne, F. Berruti, L. A. Behie, and T. J. W. De Bruijn, “The internally circulating fluidized bed (ICFB): A novel solution to gas bypassing in spouted beds,” Can. J. Chem. Eng., vol. 70, no. 5, pp. 910–915, 1992. doi: 10.1002/cjce.5450700512
[26] J. M. Lee, Y. J. Kim, and S. D. Kim, “Catalytic coal gasification in an internally circulating fluidized bed reactor with draft tube,” Appl. Therm. Eng., vol. 18, no. 11, pp. 1013–1024, 1998. doi: 10.1016/S1359-4311(98)00039-8
[27] Y. J. Kim, J. M. Lee, and S. D. Kim, “Bed With Draught Tube,” vol. 76, no. 11, pp. 1067–1073, 1997. doi: 10.1016/S0016-2361(97)00112-9
[28] J. R. Grace, Handbook of Multiphase Systems. Washington, D.C.: Hemisphere, 1982.
[29] H. T. Bi and J. R. Grace, “Effect of measurement method on the velocities used to demarcate the onset of turbulent fluidization,” Chem. Eng. J. Biochem. Eng. J., vol. 57, no. 3, pp. 261–271, 1995. doi: 10.1016/0923-0467(94)02875-B
[30] J. Kopyscinski, T. J. Schildhauer, and S. M. A. Biollaz, “Methanation in a fluidized bed reactor with high initial CO partial pressure : Part I — Experimental investigation of hydrodynamics , mass transfer effects , and carbon deposition,” Chem. Eng. Sci., vol. 66, no. 5, pp. 924–934, 2011. doi: 10.1016/j.ces.2010.11.042
[31] J. Fuchs, J. C. Schmid, S. Müller, and H. Hofbauer, “Dual fluidized bed gasification of biomass with selective carbon dioxide removal and limestone as bed material: A review,” Renew. Sustain. Energy Rev., vol. 107, no. November 2018, pp. 212–231, 2019. doi: 10.1016/j.rser.2019.03.013